forests

MDPI

Article

Disturbance Alters the Relative Importance of Topographic and Biogeochemical Controls on Microbial Activity in Temperate Montane Forests

Rebecca A. Lybrand [1,2,*], Rachel E. Gallery [2,3], Nicole A. Trahan [2] and David J. P. Moore [2]

[1] Department of Crop and Soil Science, Oregon State University, Corvallis, OR 97331, USA
[2] School of Natural Resources and the Environment, University of Arizona, Tucson, AZ 85721, USA; rgallery@email.arizona.edu (R.E.G.); nicole.trahan@gmail.com (N.A.T.); davidjpmoore@email.arizona.edu (D.J.P.M.)
[3] Department of Ecology and Evolutionary Biology, University of Arizona, Tucson, AZ 85721, USA
* Correspondence: rebecca.lybrand@oregonstate.edu; Tel.: +1-541-737-1036

Received: 7 December 2017; Accepted: 12 February 2018; Published: 24 February 2018

Abstract: Fire and pathogen-induced tree mortality are the two dominant forms of disturbance in Western U.S. montane forests. We investigated the consequences of both disturbance types on the controls of microbial activity in soils from 56 plots across a topographic gradient one year after the 2012 High Park wildfire in Colorado. Topsoil biogeochemistry, soil CO_2 efflux, potential exoenzyme activities, and microbial biomass were quantified in plots that experienced fire disturbance, beetle disturbance, or both fire and beetle disturbance, and in plots where there was no recent evidence of disturbance. Soil CO_2 efflux, N-, and P-degrading exoenzyme activities in undisturbed plots were positively correlated with soil moisture, estimated from a topographic wetness index; coefficient of determinations ranged from 0.5 to 0.65. Conversely, the same estimates of microbial activities from fire-disturbed and beetle-disturbed soils showed little correspondence to topographically inferred wetness, but demonstrated mostly negative relationships with soil pH (fire only) and mostly positive relationships with DOC/TDN (dissolved organic carbon/total dissolved nitrogen) ratios for both disturbance types. The coefficient of determination for regressions of microbial activity with soil pH and DOC/TDN reached 0.8 and 0.63 in fire- and beetle-disturbed forests, respectively. Drivers of soil microbial activity change as a function of disturbance type, suggesting simple mathematical models are insufficient in capturing the impact of disturbance in forests.

Keywords: carbon; biogeochemistry; disturbance ecology; exoenzyme activity (EEA); extracellular enzymes; fire; Mountain Pine Bark Beetle; *Ponderosa pine* (*Pinus ponderosae*); soil microbial community; SAGA wetness index; topographic wetness index; topography

1. Introduction

Forests account for half of Earth's terrestrial organic carbon (C) stocks by storing carbon as plant biomass, forest litter, and soil organic matter (SOM) [1,2]. Wildfire, insect and disease outbreaks, droughts, and other natural disasters are an integral component of forest dynamics, but changes to the frequency and severity of these disturbances world-wide present a global challenge for monitoring and managing these forests and the ecosystem services they provide [3,4]. Forests in the Western U.S. are experiencing larger wildfire disturbances attributed to warmer temperatures and earlier spring snowmelts [5], with a 60% increase in large fires from the mid-1980s in the Northern Rocky Mountains and significantly greater extents of severe fires in the Southern Rocky Mountains [6]. Furthermore, unprecedented mountain pine beetle (MPB; *Dendroctonous ponderosae*) outbreaks in Western North America killed >10 Mha of trees over the last 2–3 decades [7,8], with major impacts on

water resources [9,10], nutrient cycling [11], and forest carbon storage [12]. These disturbance-caused changes require consideration when assessing global change risks to the stability of forest carbon [13,14]. Landscape history, disturbance severity, and disturbance type represent interactive factors that reshape the composition, structure, and carbon budget of forests following disturbance events [15]. Topography also plays an integral role in the distribution of water, nutrients, and soil carbon in forested systems [16]; it is therefore likely that hillslope-scale controls would influence soil biogeochemistry and microbial activity in disturbed systems.

Wildfire disturbance in forested systems alters vegetation communities and soil biogeochemical cycling as a function of fire duration, frequency, and intensity [17]–factors that are directly or indirectly shaped by topography [18–20]. Hillslope-scale topography exerts important control on fire severity and burn frequency in Western U.S. landscapes: more frequent, low intensity wildfires occur on drier south-facing slopes in moderate drought years compared to densely vegetated north-facing slopes that experience fewer yet more severe fires during extreme drought years [20]. Organic and mineral surface soils often display similar post-fire changes in geochemistry. These include a reduction in soil organic carbon (SOC) and total nitrogen (N) through the partial to complete removal of overlying organic matter [17,21,22]; the production of inorganic nitrogen including ammonium (NH_4^+), a product of combustion, and nitrate (NO_3^-), a subsequent product of nitrification, that occurs in the days to months following a wildfire [23,24]; and the concentration of non-volatized base cations (e.g., Mg^{2+}, Ca^{2+}, K^+) into ash lost via post-fire leaching and surface runoff [25,26]. The extent of post-fire changes in soil geochemistry reflects ecosystem type, burn severity, and fire frequency [27–29], all of which are influenced by topography [30].

Forest diebacks driven by MPB outbreaks alter C and N cycling pathways to varying degrees, depending on percent tree mortality [8] and phase of infestation [9,10,31,32], among other factors. The changes in soil biogeochemistry following MPB infestation include greater soil moisture availability likely due to reduced evapotranspiration associated with high tree mortality [33]; a reduction in phosphate (PO_4^3) concentrations [34]; lower C/N ratios in the leaf litter compared to little to no change in soil C/N ratios [34]; greater aromaticity of dissolved organic carbon (DOC) [8] and elevated concentrations of NH_4^+ in the soil environment given the cessation of nitrogen uptake and more litter available following tree mortality [11,35,36]. Nitrate concentrations following MPB outbreaks vary, with the strongest NO_3^- responses in forests that receive substantial N deposition (e.g., Europe, Asia) compared to N-limited system in Western North America [37–39]. Studies of terrain-driven changes in soil biogeochemistry following MPB outbreaks are more limited, yet terrain attributes, such as slope, elevation, and aspect, serve as important factors for modeling hillslope-scale water availability following MPB outbreaks [9,10].

Microbial communities in forested systems demonstrate strong responses to disturbance-driven changes in soil geochemistry and substrate inputs in the months to years following wildfire [40,41] and MPB outbreaks [12,42]. Wildfires heat surface soils from 60 to 400 °C [43,44] and change the physical, chemical, and biological attributes of soils [45]. Fire directly impacts microbial function by reducing microbial biomass (via mortality) and changes microbial communities by filtering microbial taxa [40,46]. Fire indirectly impacts microbial function through altered substrate stoichiometry and edaphic conditions [47,48]. Over time, fire changes soil texture, bulk density, and hydrophobicity, leading to increased soil erosion and further depletion of soil SOM [23,49,50]. In contrast, microbial responses to MPB disturbance may be more driven by changes to root and organic matter inputs into soil. Mycorrhizal fungi exhibit up to a 12-fold reduction in biomass within a year of MPB-associated forest dieback coupled with an increase in the prevalence of saprotrophic fungal communities [34]. Higher bacterial/fungal biomass ratios occur in the absence of fungal-tree symbioses after tree mortality [34], which suggest that fungi and bacteria respond differently; bacterial biomass inputs remain potentially unchanged or increase in soils following MPB disturbance [12].

Forest disturbances alter rates of organic matter decomposition by microbes that introduce uncertainty to the fate of soil carbon and aboveground carbon stocks. Quantifying soil microbial

response to disturbance will reduce this uncertainty in dynamic, topographically complex ecosystems that are expected to experience greater degrees of disturbance given drought, warmer temperatures, and the lower snowpack associated with climate change [51]. Soil C, N, and phosphorus (P) biogeochemistry vary based on the time since disturbance and are contingent on moisture availability [32]. The dynamic responses of microbial enzyme activities to linked and compounded disturbance interactions requires more consideration [52], particularly in forested mountain systems where complex terrain contributes to variability in microbial responses to wildfire and MPB outbreak events.

Here, we examine how topography and two disturbance agents, wildfire and mountain pine beetle, interactively regulate soil biogeochemical responses and potential exoenzyme activities in montane forests of Colorado. Our goal is to assess how microbial functions, as indicated by soil CO_2 efflux and potential exoenzyme activities, and the resulting soil biogeochemistry in Western forested landscapes, are changed when forests are impacted by insect outbreaks, fire, and both insects and fire. We sampled 56 plots subjected to beetle disturbance from 2007 to 2009 (>90% tree mortality) and differing wildfire severity in pine-dominated forests of Colorado. Topsoil biogeochemistry, potential exoenzyme activity, and microbial biomass were quantified within each plot. We examined terrain-induced variability in moisture availability using the SAGA (System for Automated Geoscientific Analyses) wetness index generated from LiDAR-derived digital terrain models (DTMs), aspect, slope, catchment area, and solar radiation. Our sampling design incorporated combinations of beetle disturbance and fire, which allowed tests of whether microbial responses to disturbance interactions might be additive, synergistic, or negative [52]. We hypothesized that microbial activities would correlate with topography and available moisture in soils of undisturbed forests, and questioned whether this relationship would be robust to fire, insect outbreak, and the combination of both disturbances.

2. Materials and Methods

We selected three field areas in Larimer County, Colorado that spanned the High Park wildfire and previous beetle kill disturbance gradients (Figure 1): Stove Prairie Ranch (SPR), Buckhorn United Methodist Camp (UMC) and, Lory State Park (LSP). The sites are located within 15 km of each other and are situated at elevations of 2090–2435 m in the *Ponderosa pine* (*P. ponderosae* Douglas ex C.Lawson) dominated montane forest that composes about three quarters of the tree cover in the region. Douglas fir (*P. menziesii* (Mayr) Franco), quaking aspen (*P. tremuloides* Michx.) and lodgepole pine (*P. contorta* Douglas) are also present and make up an additional quarter of tree cover. The majority of precipitation falls as snow; the area receives on average 425 cm of snow with significant snowfall from October through May, peaking in April. The average annual rainfall total is 56 cm. The average air temperature is 7.8 °C (min: −7.8 °C; max: 22.2 °C) with peak monthly averages in August and September during our sampling period. All three field areas overlay the Wetmore-Boyle-Rock Outcrop Complex and consist of shallow, well to excessively drained, upland Alfisol and Mollisol soils. Soils in this complex are classified as frigid Lithic Haplustalfs and frigid shallow Aridic Argiustolls [53]. Underlying bedrock units were determined using 1:24,000 geologic quadrangle maps from the USGS (United States Geological Survey) National Map Geologic Database. All bedrock types were Precambrian (Early Proterozoic) in age, ranging from metasedimentary rocks composed of knotted mica schist at SPR to knotted mica schist and quartzofeldspathic mica schist at UMC [54]. The LSP site is underlain by Boulder Creek granodiorite and metavolcanic hornblende-plagioclase gneiss or schist interlayered with massive amphibolite [54].

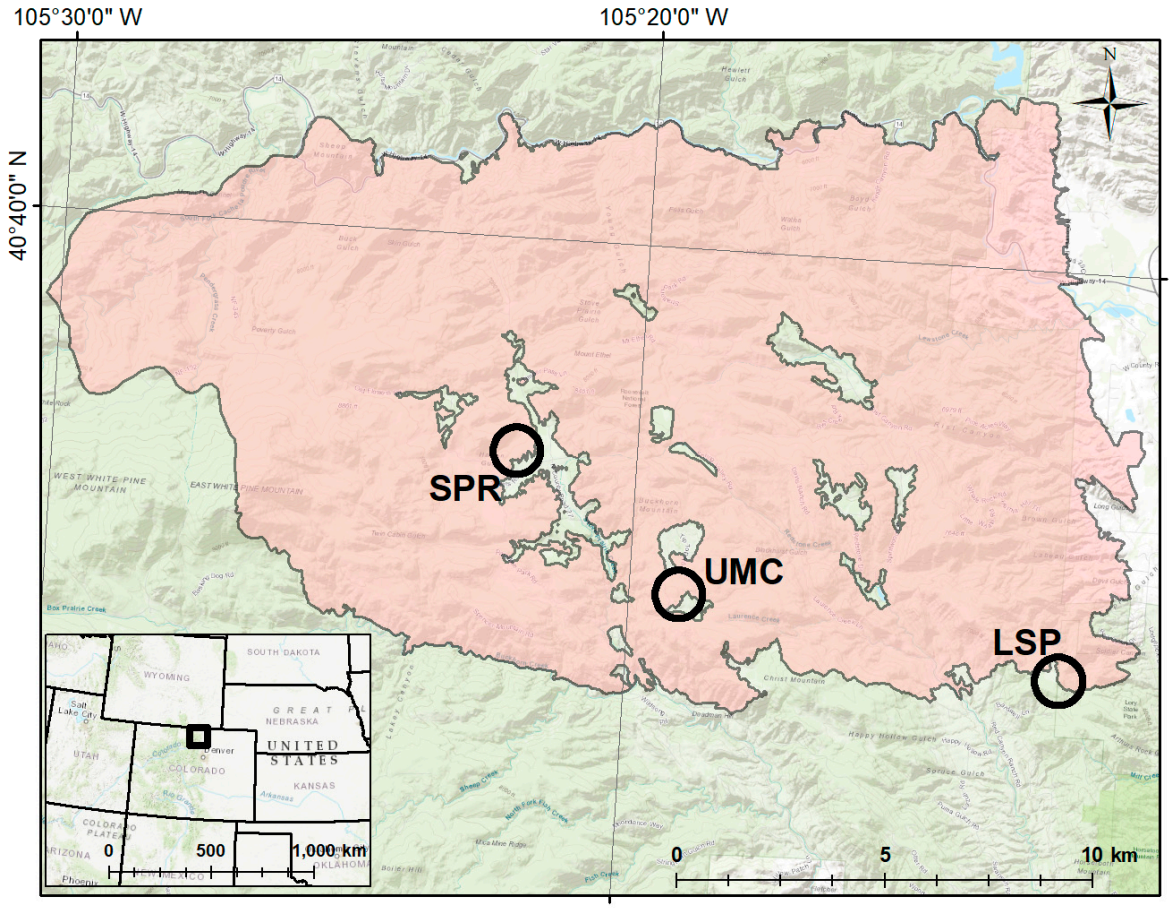

Figure 1. A map of the study area in Larimer County, CO, USA. The area burned by the 2012 wildfire is shaded red. Fifty-six study plots were established across the three study locations Stove Prairie Ranch (SPR), Buckhorn United Methodist Camp (UMC) and, Lory State Park (LSP) indicated with black circles. Inset map: the open black square contains the area of Colorado depicted by the main map.

2.1. Verification of Cause of Mortality

The High Park wildfire burned a total of 353 km^2 in June 2012, including all three field areas in our study. Despite the extensive burn perimeter, we identified areas that were unburned and burned at each study site. Prior to the wildfire, all three sites experienced patchy MPB infestation in 2007–2009. We verified the cause of mortality as follows.

To distinguish trees killed by fire from those killed by MPB, we used multi-proxy methods because, in some cases, the wildfire burned away external evidence of MPB infestation. Briefly, to locate sites where MPB and wildfire both occurred, we first created a disturbance progress map using United States Forest Service (USFS) MPB outbreak data and overlaid the High Park wildfire boundary [55]. To ascertain the location of MPB-killed trees that were affected by the High Park wildfire, we pinpointed clusters of red phase pines before the wildfire using historical aerial images on Google Earth to compare with images after the wildfire to see if they were in the wildfire zone. To confirm MPB infestation in the field, we peeled back the tree bark to reveal beetle galleries and blue stain fungus in the wood. We cored all dead trees in the candidate plots measuring >10 cm in diameter with a Haglof 5.1 mm diameter increment borer (Haglof Company Group, Langsele, Sweden). To ensure consistency and to minimize the chance of capturing growth caused by anything other than climate, such as slope, two cores per tree were taken parallel to the slope at a constant height of 1.3 m [56]. The outer ring was required to determine the year-of-death (YOD) of the tree, so care was taken to ensure that the outer ring was captured intact. Cores were labeled and stored in paper straws until analysis.

The year of death of trees killed by the MPB before the High Park wildfire in 2012 was verified using standard dendrochronological procedures [56,57]. We measured the width of each growth ring using the LINTAB tree-ring measurement station (LINTAB^{TM}5, Rinntech Inc., Heidelberg, Germany). We compiled the live tree data into a site master with known outside ring dates and crossdated the dead trees. We performed Pearson's correlation coefficient analysis ($p < 0.001$, CI = 0.3281) of ring widths in the samples and the master chronology using COFECHA 2.111 (The Laboratory of Tree Ring Research, Tucson, AZ, USA [58]). Crossdating was verified against the standardized ring-width series of the master chronology TSAP (TSAP-Win [59]; Rinntech Inc., Heidelberg, Germany [60,61]).

2.2. Establishment of Study Plots

During summer 2013, we established a total of fifty-six sampling plots across the three field sites: twenty at SPR, twenty at LSP, and sixteen at UMC (Figure 1). At each of the three field sites, we located sampling plots in four disturbance types: Burned, Beetle Present (BP, $n = 20$); Burned, Beetle Absent (BA, $n = 20$); Unburned, Beetle Present (UP; $n = 8$), and Unburned, Beetle Absent (UA, $n = 8$). In any ecological sampling scheme, spatial autocorrelation is a concern. To reduce the possibility that the sampling strategy could bias our conclusions, we established a categorical study by site by sampling disturbance plots across each of the three locations. We also indicate location (SPR, LSP, UMC) in the figures reporting the results so that any potential bias can be assessed visually. Each plot was established by placing a flag in the center of a cluster of 3–5 pines that were affected by the same disturbance type and which varied in size between 10 and 20 cm in diameter. For each plot we identified a minimum of three mature pine focal trees of each disturbance type in isolation (the edge of the plot was at least 1 m distance from any live trees or other significant vegetation or disturbance type in all directions). Working with the heterogeneity of the landscape and disturbance patterns, no plots were closer than 2 m apart and most were more than 10 m apart. Only trees above 10 cm in diameter were considered. We designated the center of the plot as the point equidistant from the focal trees. GPS coordinates, elevation for the center of the plot were recorded.

Each plot was approximately 2 m^2 in size. Locations of trees, shrubs, stumps, logs, and PVC collars (see below) were mapped within each plot to facilitate subsampling. Briefly, we designated North–South and East–West transect lines and marked these points at the plot boundary with labeled flags to create quadrants. For each tree within the plots, we measured the diameter at breast height (dbh; Forestry Suppliers Metric Fabric Diameter Tape Model 283D/5M) and heights (Suunto PM-5/360 PC Clinometer). Trees were labelled with a unique designation and disturbance status. Shrub cover was mapped but not identified to species. Finally, percent cover was estimated by two people and averaged for each quadrant.

2.3. Soil Efflux Measurements

To establish the overall metabolic activity of soils that was coincident in time with soil biogeochemical and enzyme measurements, we measured the soil CO_2 efflux from four locations within each 2 m^2 plot within 24 h of collecting samples for laboratory analysis (described below). Measurements were made prior to soil sampling for laboratory analysis between the window of 10 a.m. and 3 p.m. This is a period of stable soil efflux measurements for similar soils, with vegetation, climate and site histories in neighboring counties in CO where we have previously published studies [31,32,62].

Four PVC soil collars were installed per plot, selecting a random location in each quadrant. The location of the soil collar was at least 30 cm within the plot boundary, on relatively level ground that was free of vegetation. After 48 h, soil efflux was measured in the quadrant of each plot, using LI-COR LI-6400 infa-red gas analyzers (IRGA) equipped with 6400-09 soil CO_2 flux chambers (LI-COR Incorporated, Lincoln, NE, USA). The IRGA uses the characteristic infrared absorption of gases to measure the concentration of CO_2 building up in the chamber over time and calculates a soil efflux rate. Soil temperature in each quadrant was measured concurrently with soil efflux using the LI-COR LI-6400 thermocouple attachment, which measures temperature integrated over a depth of 0–15 cm.

IRGAs are calibrated at LI-COR every 2 two years, with the last factory calibrations in 2012. Prior to the field season IRGA zeros and spans were checked in the laboratory using tank standards.

Prior to each set of measurements, the IRGA was allowed to warm up for at least 10 min. Standard checks were made to verify pressure, water and CO_2 readings were within normal bounds. Prior to each measurement, the chamber cap was removed and the chamber was laid adjacent to the soil collar to allow the user to set the average (ambient) [CO_2] for the instrument. The soil thermocouple probe was inserted fully into the soil adjacent to the soil collar prior to the initiation of the measurement cycle. The collar depth was measured and the instrument was set such that the insertion depth was zero. In cases when it was not possible for the chamber to be flush with the surface, an insertion depth was calculated and entered into the IRGA so that the chamber volume was correctly estimated. Three efflux measurements were made at each collar using automated sampling mode for this instrument. Briefly, air was pumped through a soda lime scrub to bring the chamber CO_2 concentration to 10 ppm below the ambient [CO_2] and the rate of CO_2 build up was used to calculate the soil efflux up to 10 ppm above ambient [CO_2]. In cases where variation in efflux at a single collar exceeded 10% during a measurement cycle, data were discarded and the cycle was repeated. Soil temperature measurements were recorded simultaneously by the LI6400.

2.4. Soil Sampling, Moisture, and Biogeochemical Analysis

Within each plot, several soil samples were collected to estimate a series of different properties; nitrogen, carbon and microbial biomass and more general characteristics of the plot (pH, soil moisture, bulk density). During soil collection, litter depth and the depth of the organic layer and burn layer were evaluated visually using a plastic ruler (mm). All soil sampling was conducted while wearing nitrile gloves. Soils were homogenized, stored on ice, and returned to the laboratory to be processed within six hours. Soil was passed through a 2-mm sieve to remove debris and coarse plant material.

To calculate bulk density, we cored two randomized locations within each plot using a standard soil corer of known radius (0.7106 cm). The core length was measured and returned to the laboratory, dried at 110 °C for 48 h, and weighed to determine mass.

Approximately 200 g of burned, organic, and mineral soil was collected from the top 5 cm of two randomized locations within the plot for pH and texture. To measure pH, we used an Oakton pH Testr 3 digital pH meter (Oakton instruments, Vernon Hills, IL, USA) on a 1:1 solution of 30 g soil to 30 mL deionized water. We weighed 5 g of homogenized soil, and dried the sample in a drying oven at 60 °C for 48 h before reweighing the dried soil to calculate percent soil moisture.

To determine soil biogeochemical metrics and microbial biomass, we collected approximately 10 g soil from the top 5 cm from four randomized locations. We extracted for dissolved organic carbon (DOC), dissolved organic nitrogen (DON), and dissolved inorganic nitrogen (DIN) following established procedures [31,63]. Briefly, 25 mL of 0.5 M potassium sulfate (K_2SO_4) was added to 5 g of homogenized sample, agitated on an orbital shaker for one hour at 120 rpm and then vacuum-filtered through glass fiber filters. Concurrently, an additional 5 g of each sample was fumigated with 2 mL of ethanol-free chloroform in Erlenmeyer flask for 24 h, vented for one hour and then extracted as above to determine microbial biomass carbon and nitrogen pools. All extracts were frozen at −20 °C until analysis.

DOC and total dissolved nitrogen (TDN) in the K_2SO_4 extracts and the fumigated soil K_2SO_4 extracts were quantified using the non-purgable-organic-C protocol on a Shimadzu TOC analyzer (TOC 5000) equipped with a total dissolved nitrogen module (Shimadzu Scientific Instruments, Inc., Columbia, MD, USA). Soil microbial biomass carbon (MBC) and nitrogen (MBN) were estimated by subtracting concentrations of DOC and DON in the un-fumigated samples as well as soil free controls from the fumigated samples [64,65]. The efficiency factors for microbial biomass carbon (kEC = 0.45 [66]) and microbial biomass nitrogen (kEN = 0.54 [64]) were used to calculate the respective biomass as the difference between fumigated and non-fumigated samples.

2.5. Potential Exoenzyme Activity

We measured potential activities of seven hydrolytic enzymes: β-D-cellubiosidase (CB), α-Glucosidase (AG), β-Glucosidase (BG), and β-Xylosidase (XYL), which hydrolyze carbon-rich substrates; leucine aminopeptidase (LAP) and *N*-acetyl-β-Glucosaminidase (NAG), which hydrolyze nitrogen rich substrates, and Phosphatase (PHOS), which hydrolyzes phosphorus rich substrates. Potential exoenzyme activities were measured using a modified fluorimetric deep-well microplate technique [67]. Soil slurries were prepared with 2.75 g of soil that was stored at 4 °C for no longer than 3 weeks and 91 mL of 50 mM Tris Buffer titrated to match soil pH. Assays were run with two internal standards: dilution series (0–100 μM) of 4-methylumbelliferone (MUB) or 7-amino-4methylcoumarin (MUC) for LAP, each mixed with soil homogenate [68]. Standards for standard curves and assays were incubated at 25 °C for 1.25 and 1.5 h; 100 μL of 200 μM fluorimetric substrate was added to 900 μL of each soil slurry. Fluorescence was measured on Synergy™ 4 Multi-Mode microplate reader with an excitation wavelength of 365 nm and an emission wavelength of 450 nm. Total enzyme activities were calculated from fluorescence values as the rate of substrate converted in nmol h^{-1} g^{-1} soil [69]. We calculated specific enzyme activities as activity per unit microbial biomass C.

2.6. Terrain Analysis

Terrain attributes were calculated for each plot in the study areas using a 1-m LiDAR-derived digital surface model produced by the National Ecological Observatory Network. The 1-m digital surface model was resampled using the cubic convolution technique to eliminate microtopographic effects on the landscape and preprocessed to fill sinks [70]. Raster datasets were generated in SAGA GIS (v.2.1.4, 2014, System for Automated Geoscientific Analyses [71]) for aspect, local slope, solar radiation, catchment area, topographic wetness index, and stream power index. Aspect and local slope were produced using the Slope, Aspect, and Curvature Module whereas total, direct, and diffuse solar radiation data sets were determined from the Potential Incoming Solar Radiation Module (v.2.1.4, 2014, System for Automated Geoscientific Analyses [71]), Cary, NC, USA. Catchment area was calculated with the triangular multiple flow direction algorithm which supports multidirectional downslope flow [72]. The topographic wetness index represents putatively long-term soil moisture conditions across the study sites as determined by the likelihood that water will accumulate in or flow out of a raster cell. We calculated the *TWI* in Raster Calculator (ArcMap, v.10.2, 2014, Environmental Systems Research Institute, Redlands, CA, USA) using the SAGA-derived catchment area and slope raster imagery [73,74]:

$$TWI = \ln\left[\frac{A}{\tan(\beta)}\right] \quad (1)$$

where A is the specific catchment area and β is the local slope. High *TWIs* occur in concave, water-gathering landscapes compared to low *TWIs* which are more common for steep, convex, water-shedding hillslopes.

The stream power index (*SPI*) represents potential flow erosion at a given point on the landscape as a function of catchment area and slope [75]:

$$SPI = A \times \tan(\beta) \quad (2)$$

Higher stream power indices suggest a greater potential for erosion due to greater contributing catchment areas, higher slope gradients, and the resultant increase in water flow velocity [76].

2.7. Statistical Analyses

All statistical tests were performed on natural-log transformed data in JMP Pro (Version 13.0.0, SAS Institute, Cary, NC, USA). We employed oneway ANOVA with Tukey-Kramer (HSD) posthoc test to compare means of terrain and geochemical attributes among the 4 disturbance groupings at a 95% confidence interval. Linear regressions were used to compare potential exoenzyme activities

with dependent variables of terrain and geochemistry (e.g., SAGA wetness index; pH; geochemical ratios). We compared responses of exoenzyme activities and specific exoenzyme activities (activity per unit biomass C). There were no differences in responses and therefore only exoenzyme activities are discussed.

3. Results

3.1. Biogeochemical and Topographic Relationships by Disturbance Type

Wildfire disturbance had the largest impact on soil pH (Figure 2e), DOC/TDN (Figure 2f), N geochemistry (Figure A1), and potential exoenzyme activities, with less identifiable differences attributed to the presence or absence of MPB (Table 1). Mean soil pH was significantly higher in burned plots compared to unburned plots regardless of beetle presence. Greater NH_4^+, TDN, and NO_3^- concentrations occurred in the burned sites versus the unburned plots irrespective of MPB (Figure A1a–c), whereas biomass N was highest in unburned locations (Figure A1d). The unburned, beetle present plots exhibited the lowest NH_4^+ concentrations of the four sample groupings (Figure A1a). Soil C biogeochemistry varied little among the disturbance types, except for significantly higher DOC concentrations in burned, beetle present plots compared to beetle absent samples in both burned and unburned landscapes (Figure A2). Phosphatase (PHOS) was the only one of seven exoenzymes to exhibit significant differences by disturbance type, with lower potential activities in soils from burned, beetle absent plots compared to unburned beetle absent and beetle present plots.

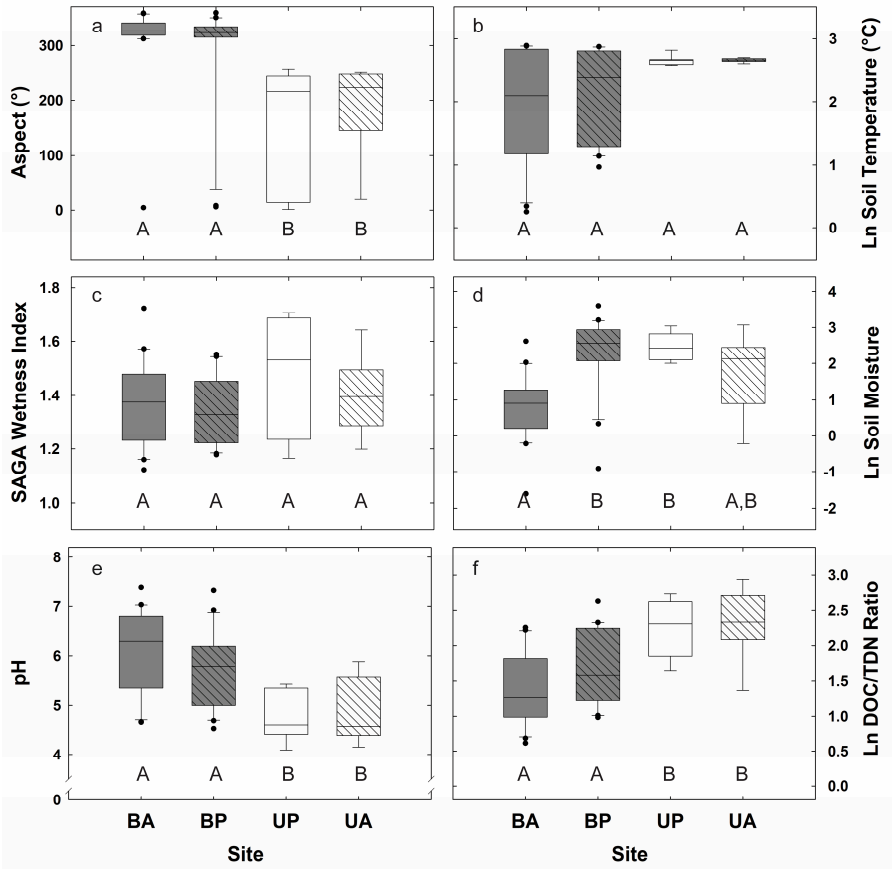

Figure 2. The four disturbance types as examined by (**a**) aspect, (**b**) soil temperature, (**c**) SAGA (System for Automated Geoscientific Analyses) wetness index, (**d**) in situ soil moisture percent, (**e**) pH, and (**f**) DOC/TDN (dissolved organic carbon/total dissolved nitrogen) ratio. Abbreviations for the disturbance types are defined as: Burned, Beetle Absent (BA); Burned, Beetle Present (BP); Unburned, Beetle Absent (UA); Unburned, Beetle Present (UP).

Aspect, or the occurrence of sites on north or south-facing hillslopes, played a role in the distribution of burned and unburned sites in our study, whereas localized surface soil moisture varied, in part, with the presence or absence of MPB. We observed that the burned plots occurred consistently on the north to northwest-facing hillslopes that receive lower influxes of average total solar radiation versus unburned landscapes with southern aspects and higher solar radiation inputs (Figure 2a,b and Figure A2a). Soil temperature did not significantly vary among the disturbance types (Figure 2b), but a one-time measure of soil moisture documented more moisture in surface soils from beetle present plots compared to beetle absent sites (Figure 2d). Specifically, plots with beetle-kill contained significantly higher surface soil moisture percentages in burned and unburned plots compared to plots where beetles were absent (Figure 2d). The SAGA wetness index did not differ among the four disturbance types as observed with aspect (Figure 2a) and total solar radiation (Figure A2b), leading to its selection as a primary terrain attribute for examining topographic control on soil CO_2 efflux, geochemistry, and potential exoenzyme activity in our study.

Table 1. Reported r^2 and *p*-values for environmental control and microbial function relationships from undisturbed and disturbed sites in Larimer County, Colorado.

Environmental Control	Microbial Function	Undisturbed		Fire		Beetles		Fire & Beetles	
		r^2	*p*-Value	r^2	*p*-Value	r^2	*p*-Value	r^2	*p*-Value
SAGA Wetness Index	Soil CO_2 Efflux	**0.68**	**0.01**	0.01	0.64	0.05	0.58	0.03	0.49
	PHOS Activity	**0.62**	**0.02**	0.00	0.88	0.33	0.13	0.00	0.98
	Sum of C Activity	0.20	0.27	0.03	0.46	0.01	0.79	0.01	0.67
	LAP Activity	**0.53**	**0.04**	0.07	0.27	**0.50**	**0.05**	0.04	0.39
	NAG Activity	**0.58**	**0.03**	0.05	0.36	0.14	0.36	0.00	0.97
pH	Soil CO_2 Efflux	0.13	0.38	0.04	0.39	0.26	0.20	0.00	0.80
	PHOS Activity	0.11	0.42	**0.80**	**<0.01**	0.18	0.27	0.11	0.15
	Sum of C Activity	0.00	0.97	**0.69**	**<0.01**	0.11	0.41	0.02	0.52
	LAP Activity	**0.92**	**<0.01**	**0.30**	**0.01**	**0.64**	**0.02**	**0.76**	**<0.01**
	NAG Activity	0.19	0.29	**0.45**	**<0.01**	0.05	0.59	0.00	0.93
DOC/TDN	Soil CO_2 Efflux	0.00	0.95	0.00	0.83	0.00	0.89	**0.28**	**0.02**
	PHOS Activity	0.21	0.25	**0.47**	**<0.01**	0.48	0.06	**0.26**	**0.02**
	Sum of C Activity	0.21	0.26	**0.51**	**<0.01**	0.02	0.74	**0.25**	**0.02**
	LAP Activity	0.02	0.77	**0.16**	**0.08**	0.06	0.55	0.05	0.34
	NAG Activity	0.14	0.36	**0.29**	**0.01**	0.52	0.05	**0.23**	**0.03**

3.2. Topographic Controls on Soil CO_2 Efflux and Potential Exoenzyme Activity

The SAGA wetness index was identified as a significant hillslope-level control in unburned, beetle absent soils that accounted for more than 50% of variability in soil CO_2 efflux and potential exoenzyme activities compared to under 10% of variability explained by this terrain attribute in burned, beetle absent soils. The SAGA wetness index for unburned, beetle absent soils exhibited strong positive relationships with soil CO_2 efflux (Figure 3a), PHOS activity (Figure 3b), NAG activity (Figure 3c), and LAP activity (Figure 3d). The SAGA wetness index did not significantly correlate with soil efflux or potential exoenzyme activities in the burned, beetle present plots, with the exception of LAP (Figure 3d). Soil C mineralizing enzyme activities and microbial biomass C did not coincide with wetness indices in either plot type (Figure 3e,f). Wetness indices from unburned, beetle present plots showed no correspondence with soil efflux or exoenzyme activities, aside for LAP, despite strong relationships among SAGA wetness index, pH, and biomass C (Table 1).

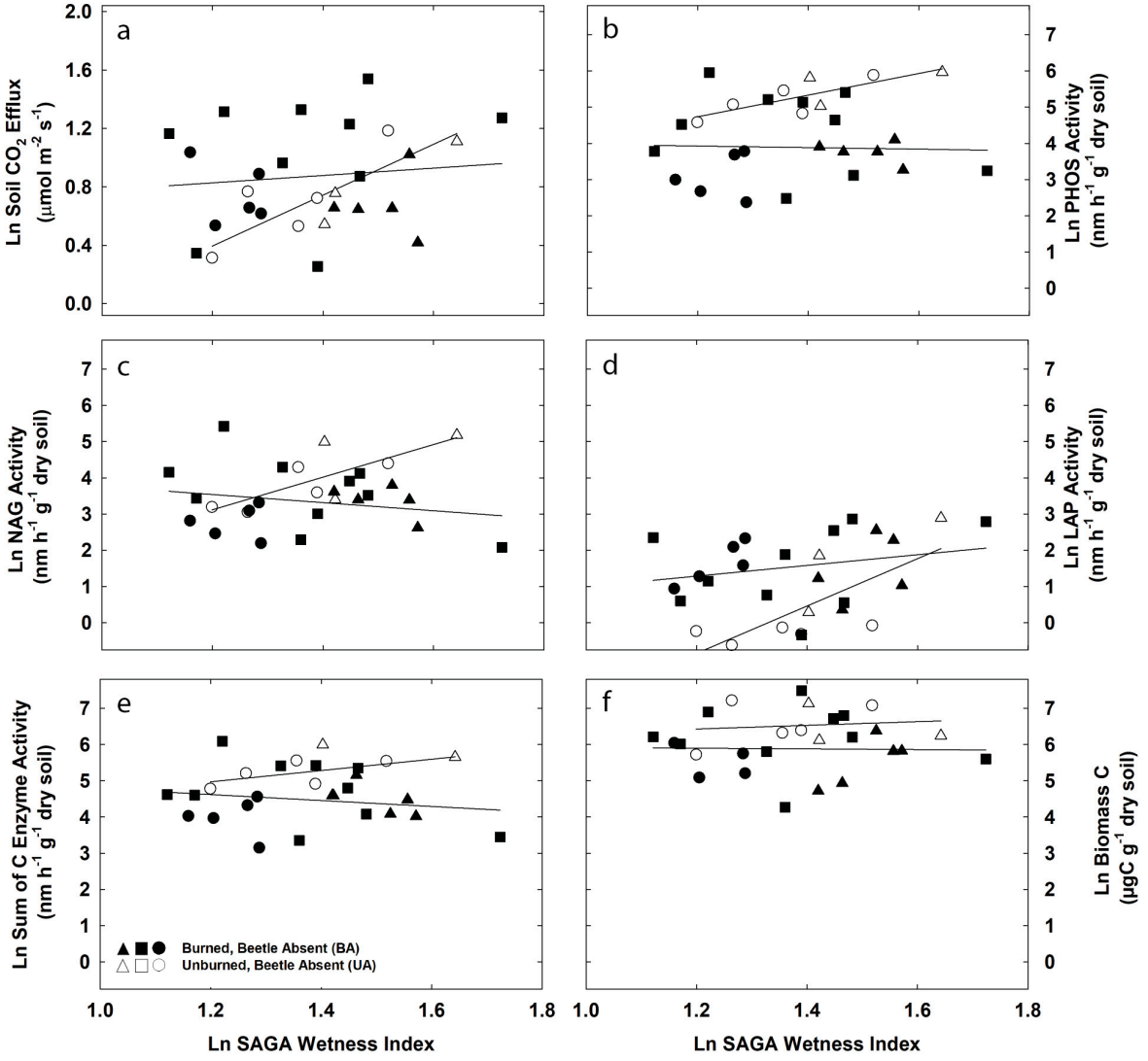

Figure 3. Burned, Beetle Absent (BA) and Unburned, Beetle Absent (UA) plots for (**a**) soil CO_2 efflux, (**b**) PHOS (Phosphatase) activity, (**c**) NAG (*N*-acetyl-β-Glucosaminidase) activity, (**d**) LAP (leucine aminopeptidase) activity, (**e**) Sum of C activities, and (**f**) Microbial Biomass C as a function of SAGA wetness index. Symbology in the figure represents data points for the following field sites: UMC (triangles), LSP (circles), and SPR (squares).

3.3. Potential Exoenzyme Activities in Fire-Disturbed Landscapes

Soil pH and DOC/TDN emerged as significant variables in burned, beetle absent plots that accounted for 30 to 80% of variability in C, N, and P potential exoenzyme activities (Figures 4a–d and 5a–d), suggesting that soil pH and geochemistry strongly influence exoenzyme activities in burned systems. Soils from burned, beetle absent plots showed strong, negative associations between pH and Sum of C activities (Figure 4a), PHOS activity (Figure 4b), and NAG activity (Figure 4c). Conversely, positive relationships occurred between soil pH and LAP activity in burned and unburned beetle absent sites (Figure 4d). DOC/TDN ratios presented positive strong relationships with Sum of C (Figure 5a), PHOS (Figure 5b), and NAG activities (Figure 5c) in burned, beetle absent plots compared to no observed relationships between DOC/TDN and exoenzyme activities in unburned, beetle absent sites (Figure 5). LAP activity did not significantly correspond to DOC/TDN in either disturbance type (Figure 5d).

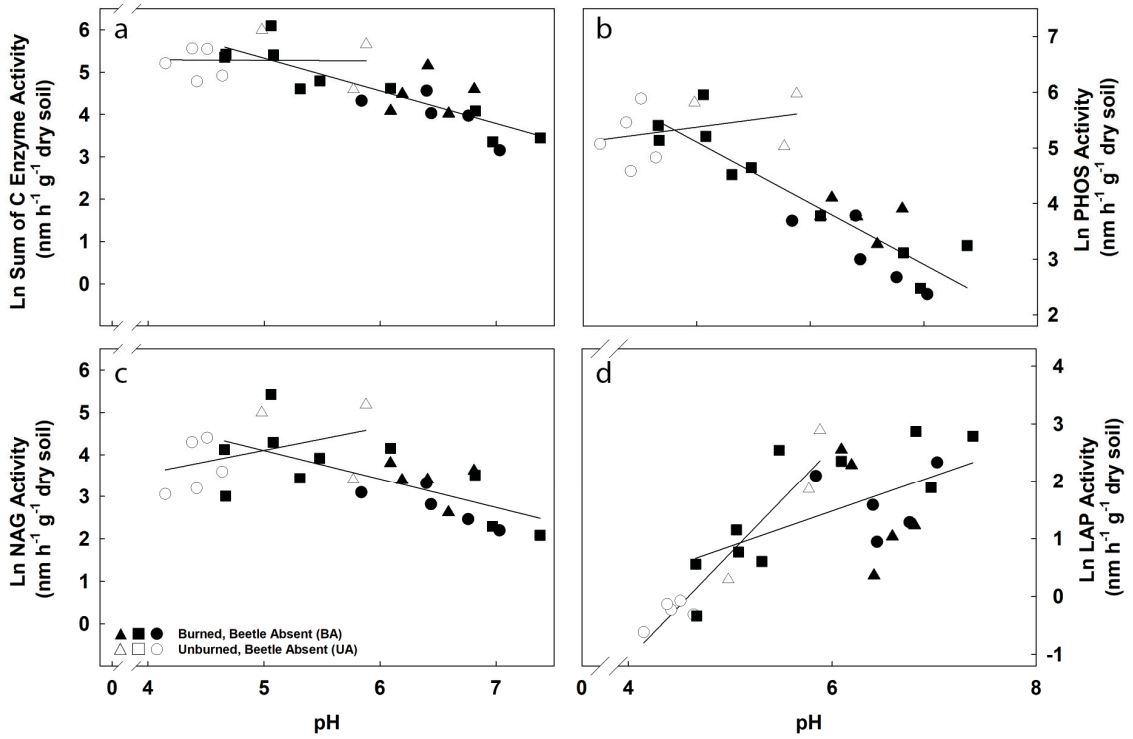

Figure 4. Burned, Beetle Absent (BA) and Unburned, Beetle Absent (UA) plots for (**a**) Sum of C activities; (**b**) PHOS activity; (**c**) NAG activity, and (**d**) LAP activity as a function of pH. Symbology in the figure represents data points for the following field sites: UMC (triangles), LSP (circles), and SPR (squares).

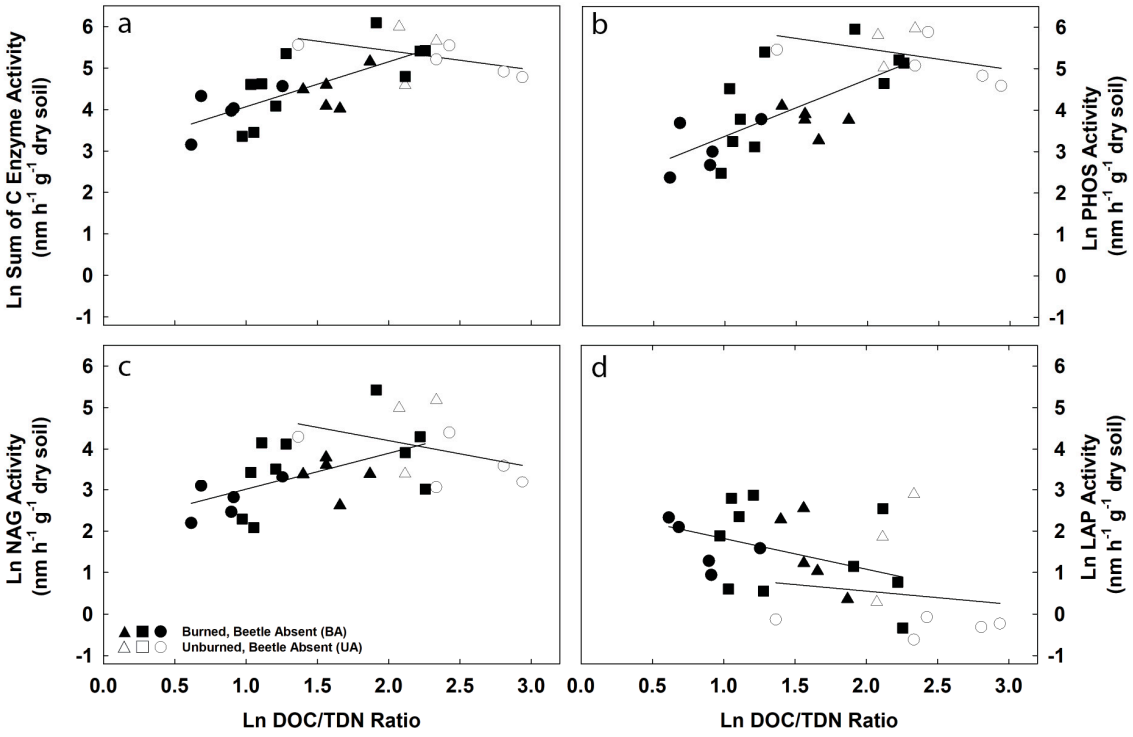

Figure 5. Burned, Beetle Absent and Unburned, Beetle Absent plots for (**a**) Sum of C EEA (exoenzyme activity); (**b**) PHOS activity; (**c**) NAG activity; and (**d**) LAP activity as a function of DOC/TDN ratios. Symbology in the figure represents data points for the following field sites: UMC (triangles), LSP (circles), and SPR (squares).

4. Discussion

Soil moisture is an important control of microbial activity in undisturbed forests. Soil CO_2 efflux along with N- and P-degrading enzymes in undisturbed forests indicated greater microbial activities in sites with higher SAGA wetness indices (Figure 3). Importantly, topography and soil moisture correlate with NPP, soil mineral nutrient, and organic matter content [77,78], with aspect playing an important role. Our unburned study sites are situated on south-facing hillslopes in low to moderate elevation forests (2090–2435 m) where moisture would be of importance. Earlier work supports this interpretation. In moderate elevation (1840–2421 m) lodgepole-dominated forests of the northern Rocky Mountains, Montana, greater seasonal CO_2 efflux in upland forest sites corresponded to soils that exhibited higher upslope accumulated areas, a proxy for lateral flow of soil water [79]. Greater fine root densities and lower C/N ratios also occurred in these wetter landscape positions that the authors attributed to greater soil CO_2 efflux and higher litter decomposition rates, respectively [79]. Soil moisture was also identified as a limiting factor for soil respiration in low to moderate elevation pine forests of Boulder Creek, Colorado, where soil CO_2 efflux corresponded to topographic wetness indices along a low to high forested elevation gradient [80]. Thus, the SAGA wetness index serves as a useful geospatial proxy for microbial activity in undisturbed forests.

In our study, conducted one year after a fire, we observed lower microbial biomass C and N in certain burned plots, and greater variability compared to undisturbed plots (Figures 2f and A1d). The plots with the lowest microbial biomass were likely where the fire was most severe. This interpretation is supported by the corresponding changes in biomass, soil pH, soil moisture, and DOC/TDN that we observed (Figure 2). Both the dominant species and the quantity of ash added to the plot after the fire would influence soil pH [81–83], variation in pH here is a reasonable proxy for fire intensity (Figure A3). At higher pH, organic compounds become more soluble and therefore more prone to leaching after wildfires in western forests [84]. As expected [23,40,49,50] pH increased (Figure 2e) and DOC declined relative to TDN (Figure 2f) in burned plots.

Fire influences microbial activity by altering soil microclimate conditions (soil temperature, soil moisture, solar insolation); soil chemistry and physical structure (pH, nutrient availability, soil structure, soil texture); and increases hydrophobicity in soils [45]. Overall, plots showing the greatest physical and biogeochemical impacts of fire displayed different microbial function from undisturbed plots (Figures 2–4). We found that, in contrast to undisturbed forest, soil CO_2 efflux and exoenzyme activities in burned plots did not correlate with the SAGA wetness index (Table 1; Figure 3b–d). The burned sites occurred on wetter, north-facing hillslopes, suggesting that microbial communities may not have experienced the same moisture limitations that result on drier south-facing sites in the unburned environments (Figure 2a). Alterations to the soil microclimate, primarily the fire-induced loss of vegetation and reduced thickness of organic soil horizons, may also explain the variability in soil temperature seen in burned sites given the potential for an increased degree of solar insolation (Figure 2b). Soil carbon and nitrogen pools change dramatically post-fire both in terms of availability and chemical structure, and microbial enzyme activity has been shown to respond to these changes to soil C/N availability both rapidly and persistently [41]. The lack of correspondence between soil moisture and microbial activities in the burned sites of our study could therefore indicate stronger control exerted by shifting nutrient limitation and microbial responses to biogeochemical properties in the burned sites (Table 1) or the influence of aspect on soil moisture conditions.

In our study, soil pH varies with fire intensity and emerges as an important explanatory variable for all exoenzyme activities, except LAP, in burned sites (Table 1; Figure 4). The pH of unburned soils was more acidic due to organic matter inputs from pine trees, whereas soils from burned forests were more alkaline but also had higher range in pH likely due to differences in burn severity (Figures 2e and 4). Soil pH represents a well-known descriptor of microbial community composition at landscape and biome scales [85–87]. Field observations of ash depth, a proxy for burn intensity was positively correlated with pH ($r = 0.7$, $p < 0.05$) and patterns of litter depth were also consistent with this interpretation (Figure A3). Associated with microbial N acquisition, LAP was positively

correlated with pH in unburned sites and remained positively correlated in burned sites (Figure 4d). A study comparing effects of fire in *Ponderosa pine* and mixed conifer forests found that, regardless of initial soil conditions, soil bacteria converged on similar community composition after severe fire [46]. Changes in substrate availability likely play a role in this shift; SOC is more soluble in basic soils [88,89]. In our study, greater fire intensity resulted in lower DOC/TDN ratios (Figure 5), which is consistent with reduced organic matter. All exoenzyme activities except LAP were positively correlated with DOC/TDN ratios (Table 1; Figure 5). Severe fires cause significant losses of SOM [90] and suggest potential greater C limitation for microbial communities in severe burn soils relative to greater N-limitation for microbial communities in less intense burns [40].

The effects of tree mortality from MPB on soil microbial function depend on the timing of beetle induced tree mortality. In contrast to the burned plots, there is no change in pH in MPB plots (Figure A3), which is consistent with several previous studies [32,36,91,92]. Unlike fire, which increases soil pH and potential for rapid leaching of soluble organic material, beetle-induced tree mortality reduces C and nutrient inputs to the soil from root exudates and litterfall in the short term, which is followed by increased C inputs from leaf, branch and root litter necromass [31,32]. Mountain Pine Beetles kill trees in association with fungi that colonize the tree when beetles bore into the phloem which disrupts transport of sugars belowground, effectively girdling the tree [90]. After tree mortality, soil extractable dissolved C and N, inorganic P and microbial biomass (C and N) decline initially but tend to increase between 4 and 5 years after tree mortality [12,32]. This loss of exudates causes increased N mineralization [32,63] and lower C/N ratios and SOC [12,31]. In this study, we see few detectable changes in the biogeochemical quantities measured (Figures 2 and A1). This is consistent with the variability we would expect, given that beetle kill occurred from 2007 to 2009 (6 to 4 years before the study); spanning the period where previous studies indicate that losses of organic inputs from live trees is transitioning to gains in organic inputs from litter decomposition [12,32]. Nevertheless, beetle disturbance still influences microbial functional controls; while PHOS, LAP and NAG are all correlated with moisture in the undisturbed plots, only LAP is statistically related to moisture in the beetle killed plots (Table 1). This might be explained by the tendency to have higher soil moisture in plots impacted by beetles (Figure 2). The regression analysis also indicates that NAG, involved with N-degradation, is correlated with the DOC/TDN ratio in beetle killed plots which contrasts with undisturbed soils. This could be because of the tendency to find higher TDN and a lower NO_3^- in the beetle killed plots compared to the undisturbed forest, indicating greater substrate availability (chitin and organic N sources) in the undisturbed forest.

Prior beetle disturbance may have modified the effect of fire on the controls of microbial activity. Soil moisture was higher in plots where beetle kill preceded fire compared to plots that were recently burned (Figure 2d). This interaction between beetle kill and fire resulted in intermediate responses of pH and DOC/TDN ratios compared to no disturbance or beetle-only plots and the plots that were burned (Figure 2e,f). We have no evidence that burn severity was lower in these plots; it is more likely that that the higher soil moisture and thicker needle layer [31,32] provided some buffering from the effects of fire (Figure A3). Exoenzyme activities were not strongly regulated by moisture in these plots, and the relationships between potential exoenzyme activities and DOC/TDN were similar to plots that experienced only fire, although soil CO_2 efflux did show a stronger response to DOC/TDN in burned sites with prior beetle disturbance compared to burned, beetle absent sites (Table 1). Also, due to the narrower range in pH, the strong relationships between exoenzyme activities and pH were absent in beetle-killed plots (Table 1).

Comparing microbial function after the fire and MPB disturbances independently and jointly allows us to evaluate whether these disturbances act in a compound manner; that the response of the second consecutive disturbance is modified by the first [52]. We have tentative support for the compound disturbance hypothesis. Both disturbances contribute enough variation to the environmental drivers of microbial function to reduce the importance of topography and its correlates as determinants of the rates of CO_2 efflux and potential enzyme activities (Table 1). While beetle

mortality alone may be complicated by the timing of when that mortality occurred [31,93,94], the environmental correlates of microbial function after fire alone (pH and DOC/TDN) are not the same as the correlates after compounded beetles and fire disturbance (DOC/TDN). In our previous work [32] and this current study, we have found limited effects of beetle mortality on soil pH itself, though we find some evidence that beetle kill apparently buffers soil pH (Figures 2e and A3). How these compound effects impact later recruitment and longer-term ecosystem function [95,96] requires longer monitoring. However, it is clear that fire does not completely erase the effects of beetle kill on microbial function and could result in longer-term changes to these ecosystems. Our analysis suggests that these disturbances are compound, rather than independent.

Montane forests recovering from historical logging and managed for some degree of fire suppression are responsible for most of the carbon uptake and storage in the Western U.S. [97,98]. Starting in the early 1990s, catastrophic levels of tree mortality have been observed across millions of hectares of bark beetle-infested forest in North America [99–101]. Forest disturbance is a fundamental driver of terrestrial carbon cycle dynamics [102], but the long-term effects of different disturbance types are poorly understood and characterized in today's land surface models [103]. Attempts to scale the impacts of different types of tree mortality remain challenging [104]. Heterotrophic function in land surface models is broadly controlled by bulk live and dead biomass, temperature, moisture, and in some cases N, and is strongly dependent on plant productivity [93,105]. Our study suggests that the environmental factors limiting microbial function shift depending on whether fire or pathogen-induced mortality is the disturbance agent. Our results are consistent with studies limited to single disturbances [31,32,40,50,92,94]. Soil biogeochemical processes can be represented through a variety of modeling approaches including a simple bulk substrate, moisture and Q10 response [105], a more complex treatment of soil substrate suitability [62,106], or even trait-based approaches [107,108]. If the type of disturbance influences biogeochemical cycling by changing availability of organic substrates and the structure or function of the microbial community, then a more complete representation of microbial processes is required.

5. Conclusions

Terrain attributes, such as the SAGA wetness index, function as useful predictors for soil CO_2 efflux and microbial activities when upscaling point analyses to watershed scales of study; however, microclimate conditions, seasonality, precipitation type, and disturbance history complicate topographic relationships with microbial activities in complex terrain. In this study, we show that the SAGA wetness index predicts exoenzyme activities in undisturbed landscapes, but that terrain-driven relationships with soil CO_2 efflux and exoenzyme activities are altered by disturbance events (e.g., fire, beetle kill) that are predicted to intensify with climate change [5,8]. Soil moisture was not a strong predictor of exoenzyme activities after both disturbance types studied here; only potential LAP activity, involved in N-degradation, was significantly correlated with the SAGA wetness index following beetle infestation (Figure 3, Table 1). Rather, pH and indicators of microbial substrate availability emerged as strong correlates of activity (Table 1; Figures 3–5). Our research demonstrates the effectiveness of using an integrated approach that combines measures of potential exoenzyme activities, soil biogeochemistry, and terrain attributes for examining the dynamic nature of heterotrophic activity and soil respiration in forest ecosystems following disturbance events. The suite of enzyme and biogeochemical assays used here enabled us to see that the breakdown of environmental drivers for soil CO_2 efflux was most likely caused by changing terrain attributes and physical and biogeochemical factors that limit the activity of the microbial community that would not be provided by soil efflux alone. Addressing soil decomposition processes in complex terrain requires that we assess the topographic, biological and biogeochemical variables that drive microbial activities, particularly in western U.S. forests where the compounded effects of wildfire and insect outbreaks are expected to increase in intensity and frequency because of global climate change.

Acknowledgments: This work was supported by an NSF RAPID (1262012) awarded to D.J.P.M. We are grateful to Emily Dynes for establishment of the experimental plots and for data collection and to M. Ross Alexander and Valerie Trouet for advice on dendrochronological techniques. R.E.G. acknowledges support from the National Science Foundation EAR 1331408 the National Institute of Food and Agriculture (NIFA ARZT-1360540-H12-199). We appreciate the constructive feedback from three anonymous reviewers. We would especially like to thank Henry Gholz for his encouragement and advice as this project developed.

Author Contributions: D.J.P.M. and N.A.T. conceived and designed the experimental design and setup; N.A.T. carried out field and laboratory analyses, R.E.G. carried out enzyme assays, R.A.L. carried out spatial and statistical analyses of the data; All authors interpreted the analyses, and R.A.L., R.E.G., and D.J.P.M. wrote the paper.

Conflicts of Interest: The authors declare no conflict of interest.

Abbreviations

α-Glucosidase (AG)	AG
β-Glucosidase (BG)	BG
carbon	C
β-D-cellubiosidase	CB
carbon dioxide	CO_2
centimeter	cm
diameter at breast height	dbh
dissolved organic nitrogen	DIN
dissolved organic carbon	DOC
dissolved organic nitrogen	DON
digital terrain models	DYM
exoenzyme activity	EEA
grams	g
infa-red gas analyzers	IRGA
Potassium sulphate	K_2SO_4
kilometers squared	km^2
leucine aminopeptidase	LAP
Lory State Park and Buckhorn	LSP
meters	m
molar	M
mountain pine beetle	MBP
million hectares	Mha
microbial biomass carbon	MBC
microbial biomass nitrogen	MBN
millimeter	mm
4-methylumbelliferone	MUB
7-amino-4methylcoumarin	MUC
Nitrogen	N
N-acetyl-β-Glucosaminidase	NAG
ammonium	NH_4^+
nanometer	nm
nitrate	NO_3^-
Net Primary Productivity	NPP
Phosphorus	P
Phosphatase	PHOS
phosphate	PO_4^3
System for Automated Geoscientific Analyses	SAGA
stream power index	SPI
soil organic carbin	SOC
soil organic matter	SOM
Stove Prairie Ranch	SPR
total dissolved nitrogen	TDN

United Methodist Camp	UMC
United States Forest Service	USFS
year of death	YOD
β-Xylosidase	XYL

Appendix

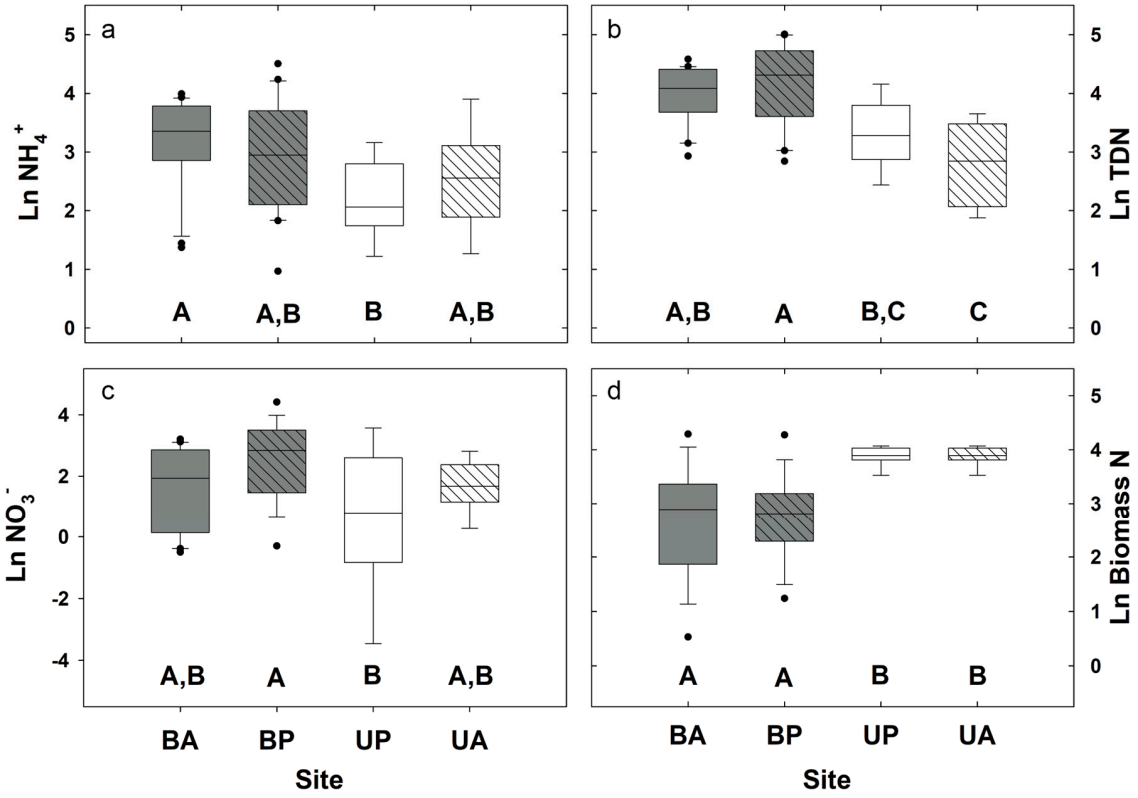

Figure A1. Nitrogen geochemistry for undisturbed and disturbed sites including (**a**) NH_4^+, (**b**) TDN, (**c**) NO_3^- and (**d**) Biomass N. Abbreviations for the disturbance types are defined as: Burned, Beetle Absent (BA); Burned, Beetle Present (BP); Unburned, Beetle Absent (UA); Unburned, Beetle Present (UP).

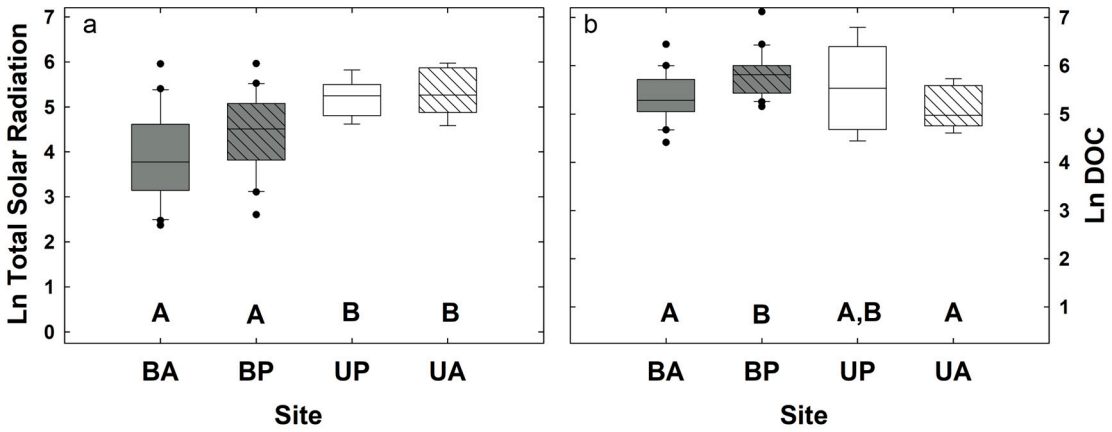

Figure A2. (**a**) Total solar radiation and (**b**) DOC concentrations among 4 disturbance groupings. Abbreviations for the disturbance types are defined as: Burned, Beetle Absent (BA); Burned, Beetle Present (BP); Unburned, Beetle Absent (UA); Unburned, Beetle Present (UP).

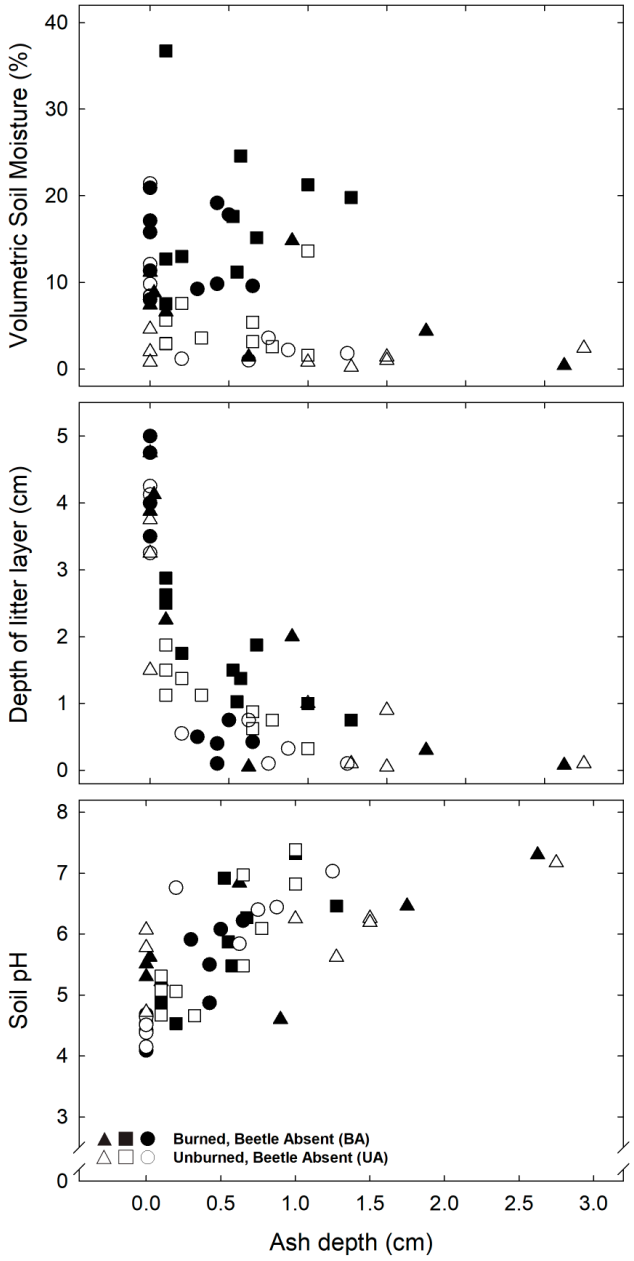

Figure A3. The relationship between volumetric soil moisture (%), litter depth (cm), soil pH and ash depth (cm) in plots with and without beetle mortality prior to the High Park fire in 2012. Symbology in the figure represents data points for the following field sites: UMC (triangles), LSP (circles), and SPR (squares).

References

1. Pacala, S.W.; Hurtt, G.C.; Baker, D.; Peylin, P.; Houghton, R.A.; Birdsey, R.A.; Heath, L.; Sundquist, E.T.; Stallard, R.F.; Ciais, P.; et al. Consistent Land- and Atmosphere-Based U.S. Carbon Sink Estimates. *Science* **2001**, *292*. [CrossRef] [PubMed]
2. Lorenz, K.; Lal, R. *Carbon Sequestration in Forest Ecosystems*, 1st ed.; Springer: Dordrecht, The Netherlands; Heidelberg, Germany; London, UK; New York, NY, USA, 2010; pp. 1–277. ISBN 978-90-481-3265-2.
3. Kautz, M.; Meddens, A.J.; Hall, R.J.; Arneth, A. Biotic disturbances in Northern Hemisphere forests—A synthesis of recent data, uncertainties and implications for forest monitoring and modelling. *Glob. Ecol. Biogeogr.* **2017**, *26*, 533–552. [CrossRef]

4. Seidl, R.; Thom, D.; Kautz, M.; Martin-Benito, D.; Peltoniemi, M.; Vacchiano, G.; Wild, J.; Ascoli, D.; Petr, M.; Honkaniemi, J.; et al. Forest disturbances under climate change. *Nat. Clim. Chang.* **2017**, *7*, 395–402. [CrossRef] [PubMed]
5. Westerling, A.L.; Hidalgo, H.G.; Cayan, D.R.; Swetnam, T.W. Warming and Earlier Spring Increase Western U.S. Forest Wildfire Activity. *Science* **2006**, *313*, 940–943. [CrossRef] [PubMed]
6. Dillon, G.K.; Holden, Z.A.; Morgan, P.; Crimmins, M.A.; Heyerdahl, E.K.; Luce, C.H. Both topography and climate affected forest and woodland burn severity in two regions of the western US, 1984 to 2006. *Ecosphere* **2011**, *2*, 1–33. [CrossRef]
7. Meddens, A.J.H.; Hicke, J.A.; Ferguson, C.A. Spatiotemporal patterns of observed bark beetle-caused tree mortality in British Columbia and the western United States. *Ecol. Appl.* **2012**, *22*, 1876–1891. [CrossRef] [PubMed]
8. Brouillard, B.M.; Mikkelson, K.M.; Bokman, C.M.; Berryman, E.M.; Sharp, J.O. Extent of localized tree mortality influences soil biogeochemical response in a beetle-infested coniferous forest. *Soil Biol. Biochem.* **2017**, *114*, 309–318. [CrossRef]
9. Mikkelson, K.M.; Dickenson, E.R.V.; Maxwell, R.M.; McCray, J.E.; Sharp, J.O. Water-quality impacts from climate-induced forest die-off. *Nat. Clim. Chang.* **2013**, *3*, 218–222. [CrossRef]
10. Mikkelson, K.M.; Bearup, L.A.; Maxwell, R.M.; Stednick, J.D.; McCray, J.E.; Sharp, J.O. Bark beetle infestation impacts on nutrient cycling, water quality and interdependent hydrological effects. *Biogeochemistry* **2013**, *115*, 1–21. [CrossRef]
11. Kana, J.; Tahovska, K.; Kopacek, J. Response of soil chemistry to forest dieback after bark beetle infestation. *Biogeochemistry* **2013**, *113*, 369–383. [CrossRef]
12. Xiong, Y.; D'Atri, J.J.; Fu, S.; Xia, H.; Seastedt, T.R. Rapid soil organic matter loss from forest dieback in a subalpine coniferous ecosystem. *Soil Biol. Biochem.* **2011**, *43*, 2450–2456. [CrossRef]
13. Van Miegroet, H.; Olsson, M. Ecosystem Disturbance and Soil Organic Carbon—A Review. In *Soil Carbon in Sensitive European Ecosystems: From Science to Land Management*; Jandl, R., Rodeghiero, M., Olsson, M., Eds.; John Wiley & Sons, Ltd.: Chichester, UK, 0255. [CrossRef]
14. Woodall, C.W.; Domke, G.M.; Riley, K.L.; Oswalt, C.M.; Crocker, S.J.; Yohe, G.W. A Framework for Assessing Global Change Risks to Forest Carbon Stocks in the United States. *PLoS ONE* **2013**, *8*, e73222. [CrossRef] [PubMed]
15. Seidl, R.; Schelhaas, M.-J.; Lexer, M.J. Unraveling the drivers of intensifying forest disturbance regimes in Europe. *Glob. Chang. Biol.* **2011**, *17*, 2842–2852. [CrossRef]
16. Tardy, Y.; Bocquier, G.; Paquet, H.; Millot, G. Formation of clay from granite and its distribution in relation to climate and topography. *Geoderma* **1973**, *10*, 271–284. [CrossRef]
17. Caon, L.; Vallejo, V.R.; Ritsema, C.J.; Geissen, V. Effects of wildfire on soil nutrients in Mediterranean ecosystems. *Earth-Sci. Rev.* **2014**, *139*, 47–58. [CrossRef]
18. Rothermel, R.C. *How to Predict the Spread and Intensity of Forest and Range Fires*; USDA Forest Service, Intermountain Forest and Range Experiment Station General Technical Report 1983, INT-GTR-143; USDA: Washington, DC, USA, 1983.
19. Taylor, A.H.; Skinner, C.N. Spatial patterns and controls on historical fire regimes and forest structure in the Klamath Mountains. *Ecol. Appl.* **2003**, *13*, 704–719. [CrossRef]
20. Bigio, E.R.; Swetnam, T.W.; Baisan, C.H. Local-scale and regional climate controls on historical fire regimes in the San Juan Mountains, Colorado. *For. Ecol. Manag.* **2016**, *360*, 311–322. [CrossRef]
21. Nave, L.E.; Vance, E.D.; Swanston, C.W.; Curtis, P.S. Fire effects on temperate forest soil C and N storage. *Ecol. Appl.* **2011**, *21*, 1189–1201. [CrossRef] [PubMed]
22. Guenon, R.; Vennetier, M.; Dupuy, N.; Roussos, S.; Pailler, A.; Gros, R. Trends in recovery of Mediterranean soil chemical properties and microbial activities after infrequent and frequent wildfires. *Land Degrad. Dev.* **2013**, *24*, 115–128. [CrossRef]
23. Certini, G. Effects of fire on properties of forest soils: A review. *Oecologia* **2005**, *143*, 1–10. [CrossRef] [PubMed]
24. Docherty, K.M.; Balser, T.C.; Bohannan, B.J.M.; Gutknecht, J.L.M. Soil microbial responses to fire and interacting global change factors in a California annual grassland. *Biogeochemistry* **2012**, *109*, 63–83. [CrossRef]
25. Ekinci, H.; Kavdir, Y. Changes in soil quality parameters after a wildfire in Gelibolu (Gallipoli) National Park, Turkey. *Fresenius Environ. Bull.* **2005**, *14*, 84–91.

26. Lasanta, A.; Cerda, A. Long-term erosional responses after fire in the Central Spanish Pyrenees: Solute release. *Catena* **2005**, *60*, 80–101. [CrossRef]
27. Santin, C.; Knicker, H.; Fernandez, S.; Menendez-Duarte, R.; Alvarez, M. Wildfires influence on soil organic matter in an Atlantic mountainous region (NW of Spain). *Catena* **2008**, *74*, 286–295. [CrossRef]
28. Turner, M.G.; Smithwick, E.A.H.; Metzger, K.L.; Tinker, D.B.; Romme, W.H. Inorganic nitrogen availability after severe stand-replacing fire in the Greater Yellowstone ecosystem. *Proc. Natl. Acad. Sci. USA* **2007**, *104*, 4782–4789. [CrossRef] [PubMed]
29. Heckman, K.; Campbell, J.; Powers, H.; Law, B.; Swanston, C. The influence of fire on the radiocarbon signature and character of soil organic matter in the Siskiyou National Forest, Oregon, USA. *Fire Ecol.* **2013**, *9*, 40–56. [CrossRef]
30. Iniguez, J.M.; Swetnam, T.W.; Yool, S.R. Topography affected landscape fire history patterns in southern Arizona, USA. *For. Ecol. Manag.* **2008**, *256*, 295–303. [CrossRef]
31. Moore, D.J.P.; Trahan, N.A.; Wiles, P.; Quaife, T.; Stephens, B.B.; Elder, K.; Desai, A.R.; Negron, J.; Monson, R.K. Persistent reduced ecosystem respiration after insect disturbance in high elevation forests. *Ecol. Lett.* **2013**, *16*, 731–737. [CrossRef] [PubMed]
32. Trahan, N.A.; Dynes, E.L.; Pugh, E.; Moore, D.J.; Monson, R.K. Changes in soil biogeochemistry following disturbance by girdling and mountain pine beetles in subalpine forests. *Oecologia* **2015**, *177*, 981–995. [CrossRef] [PubMed]
33. Clow, D.W.; Rhoades, C.; Briggs, J.; Caldwell, M.; Lewis, W.M. Responses of soil and water chemistry to mountain pine beetle induced tree mortality in Grand County, Colorado, USA. *Appl. Geochem.* **2011**, *26*, S174–S178. [CrossRef]
34. Stursova, M.S.; Snajdr, J.; Cajthaml, T.; Barta, J.; Santruckova, H.S.; Baldrian, P. When the forest dies: The response of forest soil fungi to a bark beetle-induced tree dieback. *ISME J.* **2014**, *8*, 1920–1931. [CrossRef] [PubMed]
35. Cullings, K.W.; New, M.H.; Makhija, S.; Parker, V.T. Effects of litter addition on ectomycorrhizal associates of a lodgepole pine (*Pinus contorta*) stand in Yellowstone National Park. *Appl. Environ. Microbiol.* **2003**, *69*, 3772–3776. [CrossRef] [PubMed]
36. Morehouse, K.; Johns, T.; Kaye, J.; Kaye, M. Carbon and nitrogen cycling immediately following bark beetle outbreaks in southwestern ponderosa pine forests. *For. Ecol. Manag.* **2008**, *255*, 2698–2708. [CrossRef]
37. Zimmermann, L.; Moritz, K.; Kennel, M.; Bittersohl, J. Influence of bark beetle infestation on water quantity and quality in the Grosse Ohe catchment (Bavarian Forest Forest National Park). *Silva Gabreta* **2000**, *4*, 51–62.
38. Huber, C.; Baumgarten, M.; Gottlein, A.; Rotter, V. Nitrogen turnover and nitrate leaching after bark beetle attack in mountainous spruce stands of the Bavarian forest national park. *Water Air Soil Pollut. Focus* **2004**, *4*, 391–414. [CrossRef]
39. Huber, C. Long lasting nitrate leaching after bark beetle attack in the high-lands of the Bavarian forest National Park. *J. Environ. Qual.* **2005**, *34*, 1772. [CrossRef] [PubMed]
40. Knelman, J.E.; Graham, E.B.; Trahan, N.A.; Schmidt, S.K.; Nemergut, D.R. Fire severity shapes plant colonization effects on bacterial community structure, microbial biomass, and soil enzyme activity in secondary succession of a burned forest. *Soil Biol. Biochem.* **2015**, *90*, 161–168. [CrossRef]
41. Knelman, J.E.; Graham, E.B.; Ferrenberg, S.; Lecoeuvre, A.; Labrado, A.; Darcy, J.L.; Nemergut, D.R. Rapid Shifts in Soil Nutrients and Decomposition Enzyme Activity in Early Succession Following Forest Fire. *Forests* **2017**, *8*, 347. [CrossRef]
42. Treu, R.; Karst, J.; Randall, M.; Pec, G.J.; Cigan, P.W.; Simard, S.W.; Cooke, J.E.K.; Erbilgin, N.; Cahill, J.F. Decline of ectomycorrhizal fungi following a mountain pine beetle epidemic. *Ecology* **2014**, *95*, 1096–1103. [CrossRef] [PubMed]
43. Beadle, N. Soil temperatures during forest fires and their effect on the survival of vegetation. *J. Ecol.* **1940**, *28*, 180–192. [CrossRef]
44. Bradstock, R.A.; Auld, T.D. Soil temperatures during experimental bushfires in relation to fire intensity: Consequences for legume germination and fire management in south-eastern Australia. *J. Appl. Ecol.* **1995**, *32*, 76–84. [CrossRef]
45. Hart, S.C.; DeLuca, T.H.; Newman, G.S.; MacKenzie, M.D.; Boyle, S.I. Post-fire vegetative dynamics as drivers of microbial community structure and function in forest soils. *For. Ecol. Manag.* **2005**, *220*, 166–184. [CrossRef]

46. Weber, C.F.; Lockhart, J.S.; Charaska, E.; Aho, K.; Lohse, K.A. Bacterial composition of soils in ponderosa pine and mixed conifer forests exposed to different wildfire burn severity. *Soil Biol. Biochem.* **2014**, *69*, 242–250. [CrossRef]
47. Choromanska, U.; DeLuca, T.H. Microbial activity and nitrogen mineralization in forest mineral soils following heating: Evaluation of post-fire effects. *Soil Biol. Biochem.* **2002**, *34*, 263–271. [CrossRef]
48. Dooley, S.R.; Treseder, K.K. The effect of fire on microbial biomass: A meta-analysis of field studies. *Biogeochemistry* **2012**, *109*, 49–61. [CrossRef]
49. Gonzalez-Perez, J.A.; Gonzalez-Vila, F.J.; Almendros, G.; Knicker, H. The effect of fire on soil organic matter—A review. *Environ. Int.* **2004**, *30*, 855–870. [CrossRef] [PubMed]
50. Ferrenberg, S.; Knelman, J.E.; Jones, J.M.; Beals, S.C.; Bowman, W.D.; Nemergut, D.R. Soil bacterial community structure remains stable over a 5-year chronosequence of insect-induced tree mortality. *Front. Microbiol.* **2014**, *5*. [CrossRef] [PubMed]
51. Mitton, J.B.; Ferrenberg, S.M. Mountain pine beetle develops an unprecedented summer generation in response to climate warming. *Am. Nat.* **2012**, *179*, E163–E171. [CrossRef] [PubMed]
52. Buma, B. Disturbance interactions: Characterization, prediction, and the potential for cascading effects. *Ecosphere* **2015**, *6*, 1–15. [CrossRef]
53. Soil Survey Staff, Natural Resources Conservation Service, United States Department of Agriculture. Web Soil Survey. Available online: https://websoilsurvey.sc.egov.usda.gov/ (accessed on 25 July 2017).
54. Braddock, W.A.; O'Connor, J.T.; Curtin, G.C. *U.S. Geological Survey GQ-1624, Scale 1:24,000*; Geological Survey: Reston, VA, USA, 1989.
55. Dynes, E.L. An Ecological Assessment of Mountain Pine Beetle (Dendroctonus ponderosae) and Wildfire Disturbance on Carbon Dynamics in Northwestern Colorado. Master's Thesis, University of Arizona, Tucson, AZ, USA, 2015.
56. Stokes, M.A.; Smiley, T.L. *An Introduction to Tree-Ring Dating*; University of Chicago Press: Chicago, IL, USA, 1968; ISBN 0816516804.
57. Speer, J.H. *Fundamentals of Tree Ring Research*; The University of Arizona Press, Arizona Board of Regents: Phoenix, AZ, USA, 2010; ISBN 9780816526840.
58. Holmes, R.L. Computer-assisted quality control in tree-ring dating and measurement. *Tree-Ring Bull.* **1983**, *43*, 51–67.
59. Rinn, F. *TSAP-Win: Time Series Analysis and Presentation for Dendrochronology and Related Applications*; Frank Rinn: Heidelberg, Germany, 2003.
60. Grissino-Mayer, H.D. Evaluating crossdating accuracy: A manual and tutorial for the computer program COFECHA. *Tree-Ring Res.* **2001**, *57*, 205–221.
61. Jones, E.L.; Daniels, L.D. Assessment of Dendrochronological Year-of-Death Estimates Using Permanent Sample Plot Data. *Tree-Ring Res.* **2012**, *68*, 3–16. [CrossRef]
62. Zobitz, J.M.; Moore, D.J.P.; Sacks, W.J.; Monson, R.K.; Bowling, D.R.; Schimel, D.S. Integration of process-based soil respiration models with whole-ecosystem CO_2 measurements. *Ecosystems* **2008**, *11*, 250–269. [CrossRef]
63. Weintraub, M.N.; Scott-Denton, L.E.; Schmidt, S.K.; Monson, R.K. The effects of tree rhizodeposition on soil exoenzyme activity, dissolved organic carbon, and nutrient availability in a subalpine forest ecosystem. *Oecologia* **2007**, *154*, 327–338. [CrossRef] [PubMed]
64. Brookes, P.C.; Landman, A.; Pruden, G.; Jenkinson, D.S. Chloroform fumigation and the release of soil nitrogen: A rapid direct extraction method to measure microbial biomass nitrogen in soil. *Soil Biol. Biochem.* **1985**, *17*, 837–842. [CrossRef]
65. Vance, E.D.; Brookes, P.C.; Jenkinson, D.S. An extraction method for measuring soil microbial biomass C. *Soil Biol. Biochem.* **1987**, *19*, 703–707. [CrossRef]
66. Beck, T.; Joergensen, R.G.; Kandeler, E.; Makeschin, F.; Nuss, E.; Oberholzer, H.R.; Scheu, S. An inter-laboratory comparison of ten different ways of measuring soil microbial biomass C. *Soil Biol. Biochem.* **1997**, *29*, 1023–1032. [CrossRef]
67. Wallenstein, M.D.; Haddix, M.L.; Lee, D.D.; Conant, R.T.; Paul, E.A. A litter-slurry technique elucidates the key role of enzyme production and microbial dynamics in temperature sensitivity of organic matter decomposition. *Soil Biol. Biochem.* **2012**, *47*, 18–26. [CrossRef]

68. Gebhardt, M.; Fehmi, J.S.; Rasmussen, C.; Gallery, R.E. Soil amendments alter plant biomass and soil microbial activity in a semi-desert grassland. *Plant Soil* **2017**, *419*, 53–70. [CrossRef]
69. German, D.P.; Weintraub, M.N.; Grandy, A.S.; Lauber, C.L.; Rinkes, Z.L.; Allison, S.D. Optimization of hydrolytic and oxidative enzyme methods for ecosystem studies. *Soil Biol. Biochem.* **2011**, *43*, 1387–1397. [CrossRef]
70. Planchon, O.; Darboux, F. A fast, simple and versatile algorithm to fill the depressions of digital elevation models. *Catena* **2001**, *46*, 159–176. [CrossRef]
71. Conrad, O.; Bechtel, B.; Bock, M.; Dietrich, H.; Fischer, E.; Gerlitz, L.; Wehberg, J.; Wichmann, V.; Böhner, J. System for Automated Geoscientific Analyses (SAGA) v. 2.1.4. *Geosci. Model Dev.* **2015**, *8*, 1991–2007. [CrossRef]
72. Seibert, J.; McGlynn, B.L. A new triangular multiple flow direction algorithm for computing upslope areas from gridded digital elevation models. *Water Resour. Res.* **2007**, *43*, W04501. [CrossRef]
73. Quinn, P.F.; Beven, K.J.; Chevallier, P.; Planchon, O. The prediction of hillslope flow paths for distri-buted hydrological modelling using digital terrain models. *Hydrol. Processes* **1991**, *5*, 59–79. [CrossRef]
74. Quinn, P.F.; Beven, K.J.; Lamb, R. The ln(α/tan β) index: How to calculate it and how to use it within the TOPMODEL framework. *Hydrol. Processes* **1995**, *9*, 161–182. [CrossRef]
75. Moore, I.D.; O'Loughlin, E.M.; Burch, G.J. A contour-based topographic model for hydrological and ecological applications. *Earth Surf. Processes Landf.* **1988**, *13*, 305320. [CrossRef]
76. Gruber, S.; Peckham, S. Land-surface parameters and objects in hydrology. In *Geomorphometry: Concepts, Software, Applications*; Hengl, T., Reuter, H.I., Eds.; Elsevier: Amsterdam, The Netherlands, 2009; pp. 171–194.
77. Donnegan, J.A.; Rebertus, A.J. Rates and mechanisms of subalpine forest succession along an environmental gradient. *Ecology* **1999**, *80*, 1370–1384. [CrossRef]
78. Stielstra, C.M.; Lohse, K.A.; Chorover, J.; McIntosh, J.C.; Litvak, M.; Baron-Gafford, G.; Barnard, H.; Brooks, P.D. Climatic and Landscape Influences on Soil Moisture are Primary Determinants of Soil Carbon Fluxes in Seasonally Snow covered Forest Ecosystems. *Biogeochemistry* **2015**, *123*, 447–465. [CrossRef]
79. Riveros-Iregui, D.A.; McGlynn, B.L. Landscape structure control on soil CO_2 efflux variability in complex terrain: Scaling from point observations to watershed scale fluxes. *J. Geophys. Res.* **2009**, *114*, G02010. [CrossRef]
80. Berryman, E.M.; Barnard, H.R.; Adams, H.R.; Burns, M.A.; Gallo, E.; Brooks, P.D. Complex terrain alters temperature and moisture limitations of forest soil respiration across a semiarid to subalpine gradient. *J. Geophys. Res. Biogeosci.* **2015**, *120*, 707–723. [CrossRef]
81. Raison, R.J.; McGarity, J.W. Some effects of plant ash on the chemical properties of soils and aqueous suspensions. *Plant Soil* **1980**, *55*, 339–352. [CrossRef]
82. Raison, R.J.; Keith, H.; Khanna, P.K. Effects of fire on the nutrient-supplying capacity of forest soils. *FRI Bull.* **1990**, *159*, 39–54.
83. Soto, B.; Diaz-Fierros, F. Interactions between plant ash leachates and soil. *Int. J. Wildland Fire* **1993**, *3*, 207–216. [CrossRef]
84. Ranalli, A.J. *A Summary of the Scientific Literature on the Effects of Fire on the Concentration of Nutrients in Surface Waters (No. USGS-2004-1296)*; Geological Survey: Reston, VA, USA, 2004.
85. Sinsabaugh, R.L.; Lauber, C.L.; Weintraub, M.N.; Ahmed, B.; Allison, S.D.; Crenshaw, C.; Gartner, T.B. Stoichiometry of soil enzyme activity at global scale. *Ecol. Lett.* **2008**, *11*, 1252–1264. [CrossRef] [PubMed]
86. Lauber, C.L.; Hamady, M.; Knight, R.; Fierer, N. Pyrosequencing-based assessment of soil pH as a predic-tor of soil bacterial community structure at the continental scale. *Appl. Environ. Microbiol.* **2009**, *75*, 5111–5120. [CrossRef] [PubMed]
87. Docherty, K.M.; Borton, H.M.; Espinosa, N.; Gebhardt, M.; Gil-Loaiza, J.; Gutknecht, J.L.; Gallery, R.E. Key edaphic properties largely explain temporal and geographic variation in soil microbial communities across four biomes. *PLoS ONE* **2015**, *10*, e0135352. [CrossRef] [PubMed]
88. Tavakkoli, E.; Rengasamy, P.; Smith, E.; McDonald, G.K. The effect of cation-anion interactions on soil pH and solubility of organic carbon. *Eur. J. Soil Sci.* **2015**, *66*, 1054–1062. [CrossRef]
89. Weil, R.R.; Brady, N.C. *The Nature and Properties of Soils*, 15th ed.; Pearson Education: Columbus, OH, USA, 2016; ISBN 978-0133254488.
90. Simard, D.G.; Fyles, J.W.; Pare´, D.; Nguyen, T. Impacts of clearcut harvesting and wildfire on soil nutrient status in the Quebec boreal forest. *Can. J. Soil Sci.* **2001**, *81*, 229–237. [CrossRef]

91. Griffin, J.M.; Turner, M.G. Changes to the N cycle following bark beetle outbreaks in two contrasting conifer forest types. *Oecologia* **2012**, *170*, 551–565. [CrossRef] [PubMed]
92. Keville, M.P.; Reed, S.C.; Cleveland, C.C. Nitrogen cycling responses to mountain pine beetle disturbance in a high elevation whitebark pine ecosystem. *PLoS ONE* **2013**, *8*, e65004. [CrossRef] [PubMed]
93. Edburg, S.L.; Hicke, J.A.; Lawrence, D.M.; Thornton, P.E. Simulating coupled carbon and nitrogen dynamics following mountain pine beetle outbreaks in the western United States. *J. Geophys. Res. Biogeosci.* **2011**, *116*, G04033. [CrossRef]
94. Maurer, G.E.; Chan, A.M.; Trahan, N.A.; Moore, D.J.; Bowling, D.R. Carbon isotopic composition of forest soil respiration in the decade following bark beetle and stem girdling disturbances in the Rocky Mountains. *Plant Cell Environ.* **2016**, *39*, 1513–1523. [CrossRef] [PubMed]
95. Harvey, B.J.; Donato, D.C.; Turner, M.G. Recent mountain pine beetle outbreaks, wildfire severity, and postfire tree regeneration in the US Northern Rockies. *Proc. Natl. Acad. Sci. USA* **2014**, *42*, 15120–15125. [CrossRef] [PubMed]
96. Seidl, R.; Schelhaas, M.-J.; Rammer, W.; Verkerk, P.J. Increasing forest disturbances in Europe and their impact on carbon storage. *Nat. Clim. Chang.* **2014**, *4*, 806–810. [CrossRef] [PubMed]
97. Schimel, D.; Braswell, B.H. The role of mid-latitude mountains in the carbon cycle: Global perspective and a Western US case study. In *Global Change and Mountain Regions*; Springer: Dordrecht, The Netherlands, 2005; pp. 449–456.
98. Schimel, D.; Kittel, T.G.; Running, S.; Monson, R.; Turnipseed, A.; Anderson, D. Carbon sequestration studied in western US mountains. *EOS Trans. Am. Geophys. Union* **2002**, *83*, 445–449. [CrossRef]
99. Kurz, W.A.; Dymond, C.C.; Stinson, G.; Rampley, G.J.; Neilson, E.T.; Carroll, A.L.; Ebata, T.; Safranyik, L. Mountain pine beetle and forest carbon feedback to climate change. *Nature* **2008**, *452*, 987–990. [CrossRef] [PubMed]
100. Raffa, K.F.; Aukema, B.H.; Bentz, B.J.; Carroll, A.L.; Hicke, J.A.; Turner, M.G.; Romme, W.H. Cross-scale drivers of natural disturbances prone to anthropogenic amplification: The dynamics of bark beetle eruptions. *Bioscience* **2008**, *58*, 501–517. [CrossRef]
101. Hicke, J.A.; Allen, C.D.; Desi, A.R.; Deitze, M.C.; Hall, R.J.; Hodd, E.H.; Kashian, D.M.; Moore, D.; Raffa, K.F.; Sturrock, R.N.; et al. Effects of biotic disturbances on forest carbon cycling in the United States and Canada. *Glob. Chang. Biol.* **2012**, *18*, 7–34. [CrossRef]
102. Allen, C.D.; Macalady, A.K.; Chenchouni, H.; Bachelet, D.; McDowell, N.; Vennetier, M.; Kitzberger, T.; Rigling, A.; Breshears, D.D.; Hogg, E.H.; et al. A global overview of drought and heat-induced tree mortality reveals emerging climate change risks for forests. *For. Ecol. Manag.* **2010**, *259*, 660–684. [CrossRef]
103. Running, S.W.; Nemani, R.R.; Heinsch, F.A.; Zhao, M.S.; Reeves, M.; Hashimoto, H. A continuous satellite-derived measure of global terrestrial primary production. *Bioscience* **2004**, *54*, 547–560. [CrossRef]
104. Anderegg, W.R.L.; Klein, T.; Bartlett, M.; Sack, L.; Pellegrini, A.F.A.; Choat, B.; Jansen, S. Meta-analysis reveals that hydraulic traits explain cross-species patterns of drought-induced tree mortality across the globe. *Proc. Natl. Acad. Sci. USA* **2016**, *113*, 5024–5029. [CrossRef] [PubMed]
105. Shao, P.; Zeng, X.; Moore, D.J.; Zeng, X. Soil microbial respiration from observations and Earth System Models. *Environ. Res. Lett.* **2013**, *8*, 034034. [CrossRef]
106. Bosatta, E.; Agren, G.I. Theoretical analysis of decomposition of heterogeneous substrates. *Soil Biol. Biochem.* **1985**, *17*, 601–610. [CrossRef]
107. Allison, S.D. A trait-based approach for modelling microbial litter decomposition. *Ecol. Lett.* **2012**, *15*, 1058–1070. [CrossRef] [PubMed]
108. Wieder, W.R.; Bonan, G.B.; Allison, S.D. Global soil carbon projections are improved by modelling microbial processes. *Nat. Clim. Chang.* **2013**, *3*, 909–912. [CrossRef]